In Vivo Imaging of Diacylglycerol at the Cytoplasmic Leaflet of Plant Membranes

Vermeer, J.E.M.; van Wijk, R.; Goedhart, J.; Geldner, N.; Chory, J.; Gadella, T.W.J.; Munnik, T.

DOI
10.1093/pcp/pcx012

Publication date
2017

Document Version
Final published version

Published in
Plant and Cell Physiology

License
Article 25fa Dutch Copyright Act

PCP
PLANT & CELL PHYSIOLOGY

Special Focus Issue – Regular Paper

In Vivo Imaging of Diacylglycerol at the Cytoplasmic Leaflet of Plant Membranes

Joop E.M. Vermeer[1,4,6], Ringo van Wijk[1,2], Joachim Goedhart[3], Niko Geldner[4], Joanne Chory[5], Theodorus W.J. Gadella Jr.[3] and Teun Munnik[1,2,*]

[1]Section of Plant Physiology, Swammerdam Institute for Life Sciences (SILS), University of Amsterdam, NL-1098XH, Amsterdam, The Netherlands
[2]Section of Plant Cell Biology, Swammerdam Institute for Life Sciences (SILS), University of Amsterdam, NL-1098XH, Amsterdam, The Netherlands
[3]Section of Molecular Cytology, Swammerdam Institute for Life Sciences (SILS), University of Amsterdam, NL-1098XH, Amsterdam, The Netherlands
[4]Department of Plant Molecular Biology, University of Lausanne-Sorge, Lausanne 1015, Switzerland
[5]Plant Biology Laboratory, Salk Institute for Biological Studies, La Jolla, CA 92037, USA
[6]Present address: Department of Plant and Microbial Biology, University of Zürich, Zürich 8008, Switzerland.
*Corresponding author: E-mail, T.Munnik@uva.nl; Fax, +31-205257934.
(Received September 18, 2016; Accepted January 11, 2017)

Diacylglycerol (DAG) is an important intermediate in lipid biosynthesis and plays key roles in cell signaling, either as a second messenger itself or as a precursor of phosphatidic acid. Methods to identify distinct DAG pools have proven difficult because biochemical fractionation affects the pools, and concentrations are limiting. Here, we validate the use of a genetically encoded DAG biosensor in living plant cells. The sensor is composed of a fusion between yellow fluorescent protein and the C1a domain of protein kinase C (YFP–C1a$_{PKC}$) that specifically binds DAG, and was stably expressed in suspension-cultured tobacco BY-2 cells and whole *Arabidopsis thaliana* plants. Confocal imaging revealed that the majority of the YFP–C1a$_{PKC}$ fluorescence did not locate to membranes but was present in the cytosol and nucleus. Treatment with short-chain DAG or PMA (phorbol-12-myristate-13-acetate), a phorbol ester that binds the C1a domain of PKC, caused the recruitment of the biosensor to the plasma membrane. These results indicate that the biosensor works and that the basal DAG concentration in the cytoplasmic leaflet of membranes (i.e. accessible to the biosensor) is in general too low, and confirms that the known pools in plastids, the endoplasmic reticulum and mitochondria are located at the luminal face of these compartments (i.e. inaccessible to the biosensor). Nevertheless, detailed further analysis of different cells and tissues discovered four novel DAG pools, namely at: (i) the *trans*-Golgi network; (ii) the cell plate during cytokinesis; (iii) the plasma membrane of root epidermal cells in the transition zone, and (iv) the apex of growing root hairs. The results provide new insights into the spatiotemporal dynamics of DAG in plants and offer a new tool to monitor this in vivo.

Keywords: *Arabidopsis thaliana* • Biosensor • Diacylglycerol • Phospholipase C • Tobacco BY-2.

Abbreviations: BFA, brefeldin A; DAG, diacylglycerol; DiC8, 1,2-dioctanoyl *sn*-glycerol; DGK, diacylglycerol kinase; ER, endoplasmic reticulum; EYFP, enhanced yellow fluorescent protein; IP_3, inositol 1,4,5-trisphosphate; NPC, non-specific phospholipasc C; PA, phosphatidic acid; PC, phosphatidylcholine; PE, phosphatidylethanolamine; PIP, phosphatidylinositol monophosphate; $PI(4,5)P_2$, phosphatidylinositol 4,5-bisphosphate; PKC, protein kinase C; PLC, phospholipase C; PMA, phorbol-12-myristate-13-acetate; PPI, polyphosphoinositide; PS, phosphatidylserine; TAG, triacylglycerol; TGN, *trans*-Golgi network; YFP, yellow fluorescent protein.

Introduction

Diacylglycerol (DAG) is an important intermediate in lipid metabolism and signaling. In lipid biosynthesis, DAG is a branch point between neutral storage lipids [acylation into triacylglycerol (TAG)] and its conversion into polar membrane lipids, which can be either phospholipids at the endoplasmic reticulum (ER) or glycolipids at plastids (Bruce 1998, Dörmann and Benning 2002, Benning 2009, Shimojima and Ohta 2011, Muthan et al. 2013). In signaling, DAG is typically generated through activation of the phospholipase C (PLC) pathway, which causes the minor lipid phosphatidylinositol 4,5-bisphosphate (PIP_2) to be hydrolyzed into the second messengers, DAG and inositol 1,4,5-trisphosphate (IP_3). While the latter diffuses into the cytosol where it triggers the release of Ca^{2+} from an internal store through activation of a ligand-gated calcium channel, DAG remains in the plasma membrane where it recruits and activates members of the protein kinase C (PKC) family, boosting the phosphorylation, and hence signaling, of various downstream targets. DAG also activates certain members of the TRPC (transient receptor potential, canonical) family of ion channels (Albert 2011).

While DAG and IP_3 classically act downstream of the canonical 'PLC signaling cascade' in animals, in plants this pathway is still obscure, basically because they lack homologs for PKC, TRPC and IP_3 receptors in their genomes (Munnik 2014). Nonetheless, evidence is accumulating that plants use the phosphorylated forms of DAG and IP_3 as second messengers, i.e. phosphatidic acid (PA) and inositolpolyphosphates (IPPs), such as IP_5, IP_6 and IP_7 (Arisz et al. 2009, Munnik and Vermeer

Plant Cell Physiol. 58(7): 1196–1207 (2017) doi:10.1093/pcp/pcx012, Advance Access publication on 31 January 2017, available online at www.pcp.oxfordjournals.org

2010, Testerink and Munnik 2011, Gillaspy 2013, Desai et al. 2014, Munnik 2014, Heilmann and Heilmann 2015, Heilmann 2016). Higher plants exhibit two types of DAG-generating PLCs: the 'phosphoinositide- (PI-) specific' PLC (abbreviated as PLC), which uses $PI(4,5)P_2$ and PI4P as substrate (Munnik et al. 1998a, Munnik and Testerink 2009, Munnik 2014), and the so-called 'non-specific PLC' (abbreviated as NPC), which hydrolyzes structural phospholipids such as phosphatidylcholine (PC) and phosphatidylethanolamine (PE) as substrate (Nakamura et al. 2005, Gaude et al. 2008, Nakamura et al. 2009, Wimalasekera et al. 2010, Kocourkova et al. 2011, Nakamura 2014). The Arabidopsis genome encodes nine *PLC* and six *NPC* genes. PLCs and NPCs have been implicated in diverse roles (Gaude et al. 2008, Nakamura et al. 2009, Dowd and Gilroy 2010, Peters et al. 2010, Munnik 2014, Nakamura 2014, Peters et al. 2014, Pokotylo et al. 2014, Hou et al. 2016).

Analysis of the different DAG pools in plants has been challenging. DAG is not a bilayer-forming lipid, so its levels are kept relatively low, which in Arabidopsis is approximately 1% of the polar lipids (Kaup et al. 2002, Gaude et al. 2007). Membrane isolation and fractionation procedures have identified distinct DAG pools at chloroplasts, the ER and mitochondria, i.e. all sites where lipid metabolism takes place (Dong et al. 2012, Muthan et al. 2013). A disadvantage of such analyses is that the procedures are relatively long, so DAG levels and pools can easily change due to modifying enzymes or transporters present in the various membrane fractions (Muthan et al. 2013). To map DAG pools in plastids, Benning's lab recently generated transgenic Arabidopsis lines expressing a DAG kinase (DGK) from *Escherichia coli*, which was targeted to the different leaflets of the chloroplast envelope membranes (Muthan et al. 2013). By comparing whole-tissue lipid profiles, each of the transgenic lines was found to exhibit a distinct pattern of DAG, PA, PC and TAG steady-state levels, supporting a separate function for DAG in each leaflet. Alternatively, isotopic tracers have been used to measure DAG pools. For example, [^{14}C]glycerol and [^{14}C]acetate labeling studies in developing embryos could distinguish at least two, possibly three distinct DAG pools (Bates et al. 2009). Although their subcellular localization remained unknown, the majority of this DAG was speculated to be associated with oil bodies for TAG synthesis and with ER subdomains for the assembly of PC and PE (Bates et al. 2009).

A DAG pool that would be generated through PLC hydrolysis of polyphosphoinositides (PPIs) is also expected to be low since the concentration of these minor lipids is $<0.5\%$ of the total phospholipid pool, which is $<0.1\%$ of all glycerolipids (Munnik et al. 1994, Munnik et al. 1998a). In mammalian cells and in the green algae *Chlamydomonas* and *Dunaliella*, PIP and PIP_2 levels are approximately equal, but in flowering plants, PIP_2 amounts are approximately 20- to 100-fold lower (Munnik et al. 1998a, Munnik et al. 1998b, Meijer and Munnik 2003, Munnik 2014). The reason for this is unknown, but a constitutively active PLC continuously hydrolyzing $PI(4,5)P_2$ into DAG and IP_3 has been one of the speculations (Munnik et al. 1998a, Mueller-Roeber and Pical 2002, van Leeuwen et al. 2007, Munnik 2014). The location of this DAG pool is expected to be at the plasma membrane where PLC activity and the kinases that make PIP and PIP_2 are localized (Munnik et al. 1998a, Mueller-Roeber and Pical 2002, Heilmann 2008a, Heilmann 2008b, Ischebeck et al. 2010, Munnik and Nielsen 2011, Pokotylo et al. 2014, Heilmann 2016), but basically this has never been addressed (Arisz et al. 2000, Heilmann 2008a, Xue et al. 2009, Ischebeck et al. 2010, Boss and Im 2012, Dong et al. 2012).

One of the exciting developments in cell biology has been the ability to visualize certain lipids in vivo using so-called 'lipid biosensors', i.e. fusions of a fluorescent protein to a lipid-binding domain specific for a particular lipid (Vermeer and Munnik 2013). When the concentration of this lipid is below the detection level, the probe will be in the cytosol (and often in the nucleus too due to its free diffusion). However, when the concentration of the lipid is high enough, or increases in response to stimulation, then the biosensor will bind the lipid and locate the membrane where the lipid is formed. Obviously, this method only detects lipids at the cytoplasmic leaflet of membranes, but the advantage is that it can reveal its subcellular localization in vivo, in real time, and disclose dynamics that otherwise would have remained hidden. In the mammalian field, such lipid biosensors have been a great success (Hammond and Balla 2015). Similarly, for the plant field, four distinct lipid biosensors have successfully been characterized, i.e. for $PI(4,5)P_2$ (Vincent et al. 2005, van Leeuwen et al. 2007, Simon et al. 2014), PI4P (Thole et al. 2008, Vermeer et al. 2009, Simon et al. 2014), PI3P (Voigt et al. 2005, Vermeer et al. 2006, Simon et al. 2014) and phosphatidylserine (PS) (Yamaoka et al. 2011).

Here, we describe and validate a biosensor that monitors DAG. It consists of a fusion between the yellow fluorescent protein (YFP) and the cysteine-rich 1a (C1a) domain of human PKCγ that specifically binds DAG and has been extensively characterized in mammalian cells (Oancea et al. 1998, Kim et al. 2011). The probe has been used in tobacco pollen tubes previously, but in that study only transient expression using a pollen-specific promoter after particle bombardment was reported, and DAG binding was never validated (Helling et al. 2006). Here we used transient expression of the DAG biosensor in cowpea protoplasts and also stably expressed it in two model systems, i.e. tobacco BY-2 cells and *Arabidopsis thaliana* plants. DAG binding was validated using a short-chain analog and PMA (phorbol-12-myristate-13-acetate), a phorbol ester that mimics DAG binding to the C1a domain and in animal cells activates PKC (Oancea et al. 1998). We found that the biosensor was mostly localized in the cytosol, indicating that the concentration of DAG in the cytoplasmic leaflet of membranes is normally too low to be detected by YFP–$C1a_{PKC}$. Detailed further analysis, however, revealed four novel DAG pools: one at the cytoplasmic leaflet of Golgi membranes and three very local and temporal pools at the plasma membrane, i.e. in root epidermal cells of the transition zone, in dividing cells at the growing cell plate and during polarized tip growth in root hairs. The results provide new insights into the spatiotemporal dynamics of plant DAG and offers a new tool to monitor this in vivo.

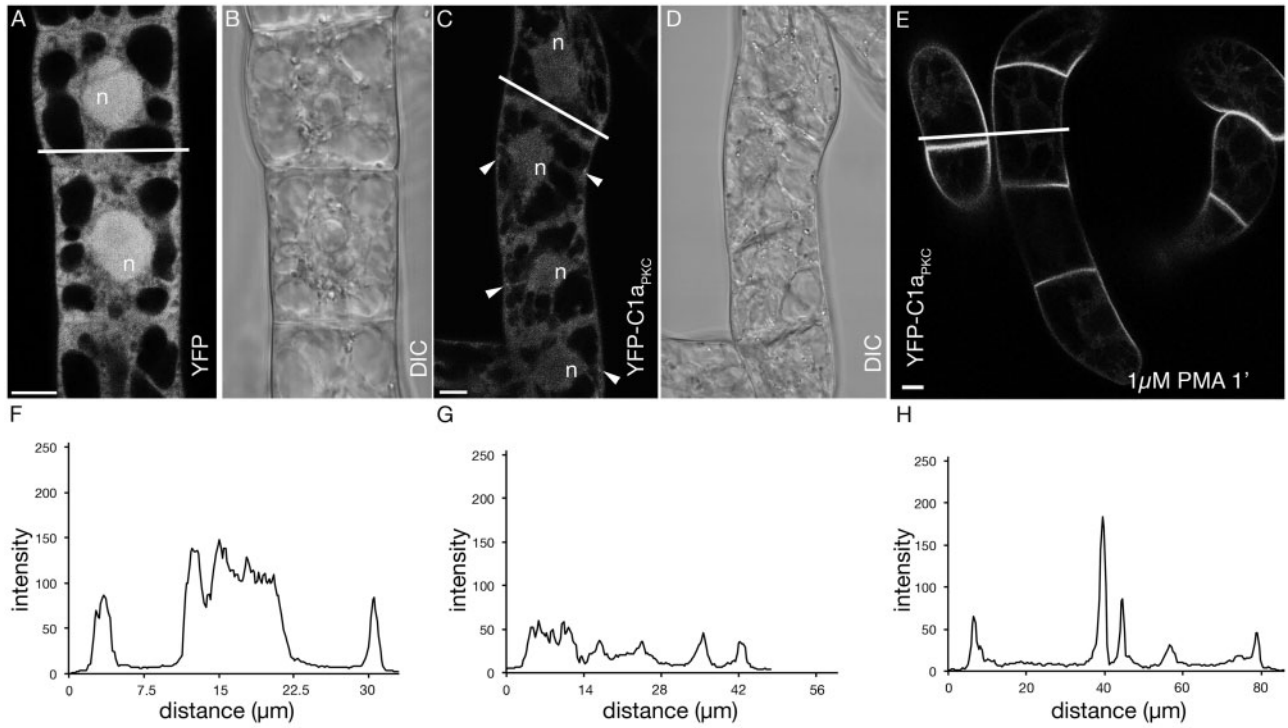

Fig. 1 Stable expression of the DAG biosensor, YFP–C1a$_{PKC}$, in tobacco BY-2 cells. Confocal images of tobacco BY-2 cells expressing (A, B) free YFP, (C, D) YFP–C1a$_{PKC}$ or (E) YFP–C1a$_{PKC}$ after treatment with the DAG analog PMA. Free YFP shows cytosolic and nuclear fluorescence, whereas YFP–C1a$_{PKC}$ shows additional labeling of punctate structures in the cytosol. (E) Treatment of the BY2 cells with 1 μM PMA results in fast accumulation of YFP–C1a$_{PKC}$ at the plasma membrane. (F–H) Intensity plot profiles of YFP fluorescence along with the line as indicated in (A), (C) and (E) to reveal strong accumulation of YFP fluorescence at the plasma membrane after PMA treatment (H) compared with the control (F, G). Arrowheads in (C) indicate YFP–C1a$_{PKC}$-labeled punctate structures. The nucleus is indicated by (n). (A), (C) and (E) show YFP fluorescence and (B) and (D) show differential interference contrast (DIC). Scale bars = 10 μm.

Results

YFP–C1a$_{PKC}$ localization in tobacco BY-2 cells

In mammalian cells, YFP–C1a$_{PKC}$ has been shown to function as a robust DAG biosensor (Oancea and Meyer 1998, Oancea et al. 1998). To investigate its use in plant cells, stable transgenic tobacco BY-2 cells were generated that expressed YFP–C1a$_{PKC}$ under the control of the constitutive 35S promoter. As shown in **Fig. 1**, most of the YFP–C1a$_{PKC}$ fluorescence was localized in the cytosol and nucleus, like YFP alone (**Fig. 1**). Nonetheless, some signal was present as motile, punctate structures (arrowheads in **Fig. 1**), but no clear plasma membrane signal was visible. To test the functionality of the DAG biosensor, the phorbol ester PMA was tested. PMA mimics the binding of DAG to the C1a domain and is therefore a potent activator of PKC activity in vivo and causes a rapid recruitment of YFP–C1a$_{PKC}$ to the plasma membrane of animal cells (Oancea and Meyer 1998, Oancea et al. 1998). Treatment of our tobacco YFP–C1a$_{PKC}$ cells with 1 μM PMA also resulted in a strong relocalization of the biosensor to the plasma membrane (**Supplementary Fig. S1**). As a second control, we tested a short-chain analog of DAG, i.e. 1,2-dioctanoyl *sn*-glycerol (DiC8), which has the advantage of being water soluble compared with normal DAG. While DiC8 failed to induce a relocalization of the biosensor in BY-2 cells (data not shown), it did trigger the relocation of YFP–C1a$_{PKC}$ to the plasma membrane of cowpea protoplasts in a fashion similar to that of PMA (**Supplementary Fig. S2**). Most probably, the DiC8 gets stuck in the cell wall. Together these results indicate that YFP–C1a$_{PKC}$ monitors DAG in the cytoplasmic leaflet of plant membranes in vivo, but that the basal concentrations of such pools are relatively low.

DAG dynamics during cytokinesis in BY-2 cells

During cytokinesis, distinct labeling patterns and dynamics for PI3P, PI4P and PI(4,5)P_2 biosensors were found in tobacco BY-2 cells. For example, PI3P was always present on punctate structures that surrounded the cell plate like a donut structure but was never part of the cell plate (Vermeer et al. 2006). In contrast, the PI4P biosensor labeled the cell plate right from the start of its formation (Vermeer et al. 2009), while the PI(4,5)P_2 biosensor only labeled the leading edges of the growing cell plate (van Leeuwen et al. 2007). Hence, we decided to follow the dynamics of the DAG biosensor during cytokinesis.

Following cell divisions in the YFP–C1a$_{PKC}$ BY-2 cell line, we found that the biosensor labeled the newly formed cell plate right up until fusion with the parental plasma membrane occurred (**Fig. 2**; **Supplementary Movie S1**). Co-labeling with the endosomal tracer FM4-64 suggested that the YFP–C1a$_{PKC}$ appeared only slightly later (**Fig. 2**; **Supplementary Movie S2**),

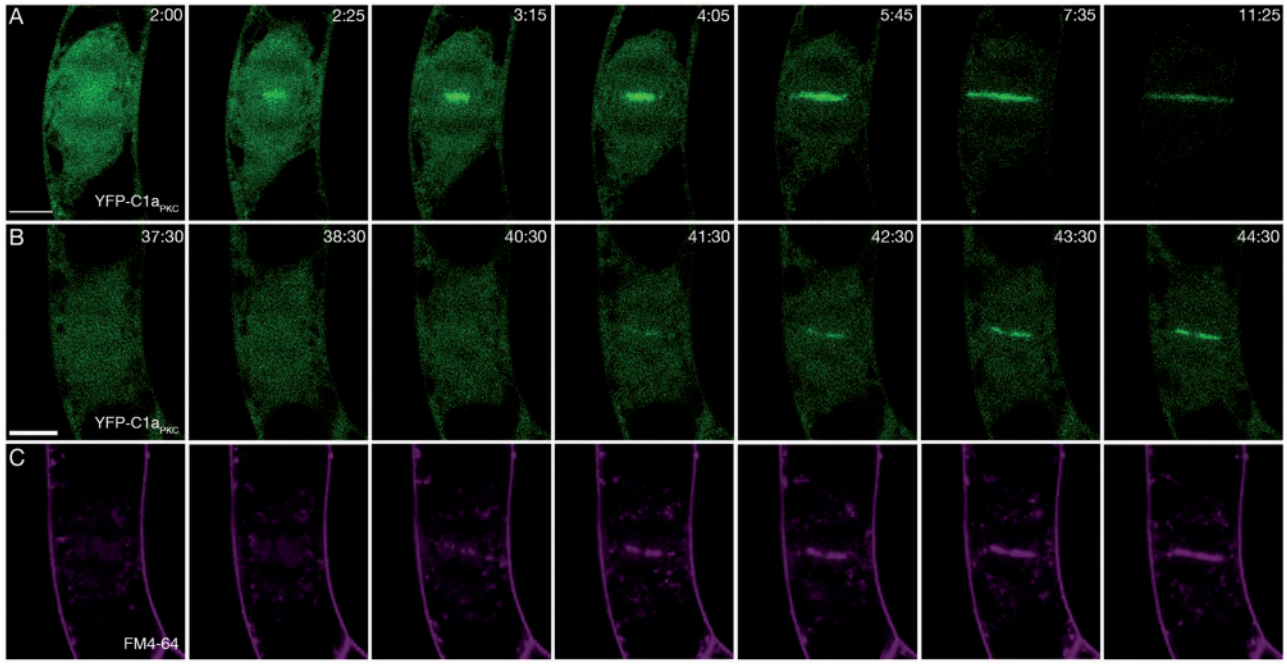

Fig. 2 YFP–C1a$_{PKC}$ accumulates at the cell plate during cell division. (A) Confocal time-lapse images of a dividing BY-2 cell expressing YFP–C1a$_{PKC}$, labeling the cell plate during all stages of its formation and growth. (B, C) Confocal time-lapse images of a dividing BY-2 cell expressing YFP–C1a$_{PKC}$ (green) co-labeled with 2 μM FM4-64 (magenta). The time series indicates that FM4-64 reaches the cell plate slightly earlier than the DAG biosensor. Time is indicated in minutes and corresponds to **Supplementary Movies S1** (A) and S2 (B, C). Scale bar = 10 μm.

which is reminiscent of what we observed for PI4P (Vermeer et al. 2009). These results indicate that during cell division, relatively high amounts of DAG are formed.

Localization of YFP–C1a$_{PKC}$ in Arabidopsis seedlings

In order to image DAG dynamics in whole plants, we generated transgenic Arabidopsis lines that expressed 35S-EYFP–C1a$_{PKC}$. To increase the avidity of the biosensor, we also generated lines that expressed two C1a domains in tandem (EYFP–2 × C1a$_{PKC}$). Such an approach has had success before to monitor PI3P and PI(4,5)P_2, whose concentrations are also very low (Vermeer et al. 2006, Simon et al. 2014). To avoid potential problems due to the strong activity of the 35S promoter, we also generated lines expressing the DAG biosensor under the control of the UBQ10 promoter. This drives stable and lower levels of expression, which are still sufficient for confocal microscopy (Geldner et al. 2009). At least 6–10 independent lines were analyzed and all showed similar localization patterns. Importantly, all lines appeared and grew like wild-type plants (**Supplementary Fig. 3**).

In **Fig. 3**, a typical fluorescence pattern of UBQ10::EYFP, 35S::EYFP–C1a$_{PKC}$, UBQ10::EYFP–C1a$_{PKC}$ and UBQ10::EYFP–2 × C1a$_{PKC}$ in the epidermis of roots of 5-day-old Arabidopsis seedlings is shown. Unlike free YFP that is located in the cytosol and nucleus, YFP–C1a$_{PKC}$ fluorescence was found in punctate structures that were also observed in the tobacco BY-2 cells expressing the DAG biosensor (**Fig. 3A–L**). Interestingly, in the epidermis of the transition zone of the primary root, we could now also detect some YFP–C1a$_{PKC}$ labeling at the plasma membrane (**Fig. 3**). Although the UBQ10::EYFP–C1a$_{PKC}$ lines showed much weaker fluorescence compared with the 35S line, the observed labeling pattern was very similar (**Fig. 3B, C**). The UBQ10::EYFP–2 × C1a$_{PKC}$ lines displayed a similar localization pattern, but with a much stronger labeling of both punctate structures and the plasma membrane (**Fig. 3D, J**). This is likely to be due to the higher avidity of this biosensor. Interestingly, the plasma membrane localization of the biosensor gradually disappeared as the epidermal cells started to elongate (**Fig. 3D–F**, J–L). Western blot analysis of the lines expressing the different biosensors indicated that most of the fusion protein was intact and had the predicted size (**Supplementary Fig. S4**). Differentiated root cell types and leaf pavement cells revealed similar fluorescence patterns of YFP–C1a$_{PKC}$ and YFP–2 × C1a$_{PKC}$, although we did not observe labeling of the plasma membrane (**Supplementary Fig. S5**).

To validate DAG binding, we also generated plants expressing a fluorescent protein fused to the C1a$_{PKC}$ domain carrying a P46G mutation, which is essential for DAG binding (Oancea et al. 1998). As shown in **Supplementary Fig. S6**, mCherry–C1a$_{PKC\text{-}P46G}$ was localized in the cytosol of root epidermal cells and root hairs. Upon PMA treatment, it no longer translocated to the plasma membrane while the intact EYFP–C1a$_{PKC}$ did. These data support that the observed localization pattern of EYFP–C1a$_{PKC}$ is dependent on its lipid-binding capacity.

YFP–C1a$_{PKC}$ reveals a pool of DAG at the *trans*-Golgi network

In mammalian cells, small amounts of DAG have been reported to reside at the *trans*-Golgi network (TGN) where it is involved

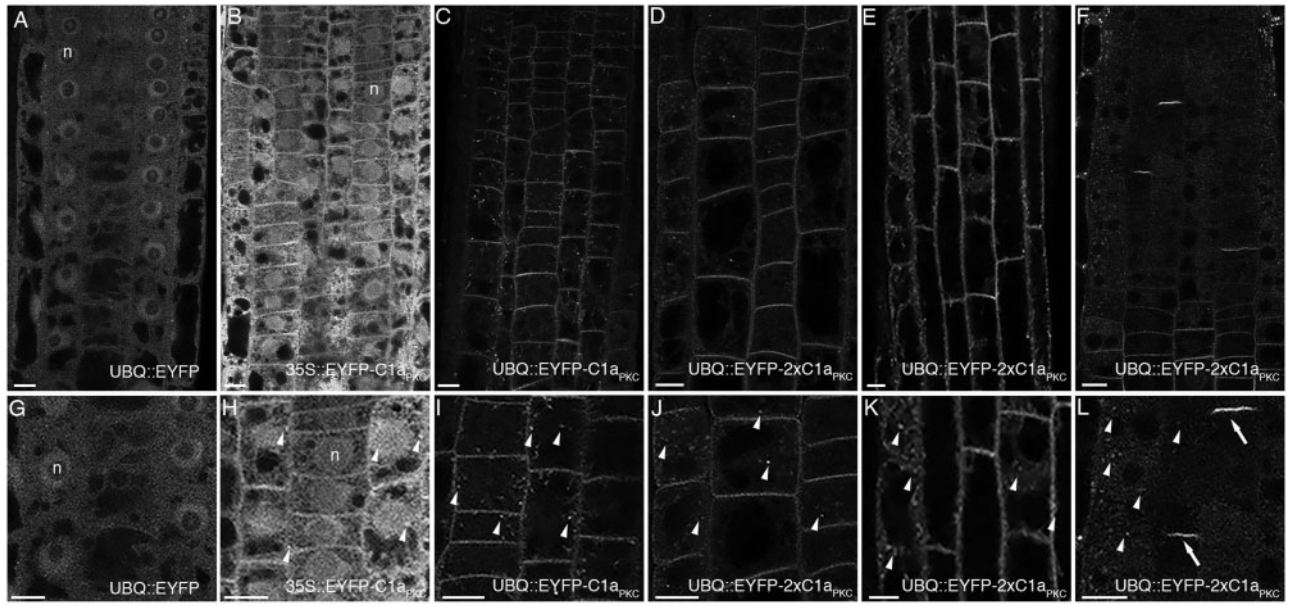

Fig. 3 Localization of different DAG biosensors in Arabidopsis seedlings. Confocal fluorescence images of various tissues of 5-day-old Arabidopsis seedlings expressing free YFP (A, G), 35S::YFP–C1a$_{PKC}$ (B, H), UBQ10::EYFP–C1a$_{PKC}$ (C, I) and UBQ10::EYFP–2 × C1a$_{PKC}$ (D–F and J–L). Whereas free YFP is localized in the cytosol and nucleus, YFP–C1a$_{PKC}$ and YFP–2 × C1a$_{PKC}$ also display labeling of the plasma membrane and punctated structures [indicated by arrowheads in (H–L)]. (F and L) YFP–2 × C1a$_{PKC}$ labeling of newly formed cell plates [arrows in (L)]. (D and E) Transient labeling of the plasma membrane by YFP–2 × C1a$_{PKC}$ that disappears when cells start elongating. (G–L) Magnification of (A–H). YFP fluorescence is shown in gray. The nucleus is indicated by (n), Scale bars = 10 μm.

in membrane fission to form transport carriers (Yeaman et al. 2004, Bossard et al. 2007). To investigate the identity of the punctate structures that we observed, plants expressing YFP–C1a$_{PKC}$ were crossed with UBQ10::mCherry–RabA1g and with the PI4P biosensor 35S::mRFP–PH$_{FAPP1}$. RabA1g accumulates at the TGN, while mRFP–PH$_{FAPP1}$ also labels, in addition to the plasma membrane, Golgi membranes (Geldner et al. 2009, Vermeer et al. 2009, Simon et al. 2014). As is clear from **Fig. 4**, a partial co-localization between YFP–C1a$_{PKC}$ and both Golgi markers was observed.

The fungal toxin brefeldin A (BFA) has been shown to inhibit Golgi trafficking and to induce the appearance of large, so-called BFA compartments (Geldner et al. 2003). BFA treatment (50 μM, 45 min) resulted in a strong accumulation of both YFP–C1a$_{PKC}$ and RabA1g in BFA compartments (**Fig. 4**), again suggesting that YFP–C1a$_{PKC}$ detects DAG at the TGN. As was reported previously, mRFP–PH$_{FAPP1}$ labeled structures that were much more resistant to BFA treatment and only showed a weak accumulation in BFA compartments (**Fig. 4**). BFA treatment of UBQ10::EYFP–C1a$_{PKC}$ and UBQ10::EYFP–2 × C1a$_{PKC}$ seedlings co-incubated with FM4-64 (a fluorescent lipophilic membrane dye) also revealed a clear accumulation of both YFP and FM4-64 signal in BFA compartments (**Supplementary Fig. S7**).

YFP–C1a$_{PKC}$ accumulates at the tip of growing root hairs

When analyzing growing root hairs, a polar localization of the YFP–C1a$_{PKC}$ signal was observed, which changed during development (**Fig. 5**). In young root hairs establishing tip growth, YFP–C1a$_{PKC}$ was localized to the apex of the root hair, whereas in older root hairs that had fully established tip growth, YFP–C1a$_{PKC}$ labeled the shanks of the root hair, just below the apex, but also faintly a compartment just below the tip of the growing root hair (**Fig. 5**). This localization pattern resembled that of the TGN-localized small GTPase, AtRABA4b (Preuss et al. 2006, Kang et al. 2011) and may indicate that DAG is involved in membrane trafficking required for the polar growth of root hairs. Interestingly, EYFP–2 × C1a$_{PKC}$ showed a much stronger plasma membrane localization, which could already be detected during bulge formation (**Fig. 5**). During establishment of tip growth, EYFP–2 × C1a$_{PKC}$ shifted its plasma membrane localization from the apex to the shanks (**Fig. 5**; **Supplementary Movie S3**).

Discussion

Using YFP–C1a$_{PKC}$ as a biosensor to visualize DAG in living plant cells

In mammalian cells, YFP–C1a$_{PKC}$ is a well-established biosensor for imaging the localization and dynamics of DAG (Oancea and Meyer 1998, Oancea et al. 1998, Kim et al. 2011). In this study, its potential to image DAG in two well-established plant systems is described, i.e tobacco BY-2 cells and Arabidopsis seedlings.

Confocal imaging revealed that most of the YFP–C1a$_{PKC}$ fluorescence was located in the cytosol and nucleus; a pattern that is similar to cells expressing YFP alone (**Figs. 1**, **3**). However, PMA, a phorbol ester that mimics DAG binding, and a short-chain analog of DAG (DiC8) were both able to relocate the biosensor to the plasma membrane (**Supplementary Figs.**

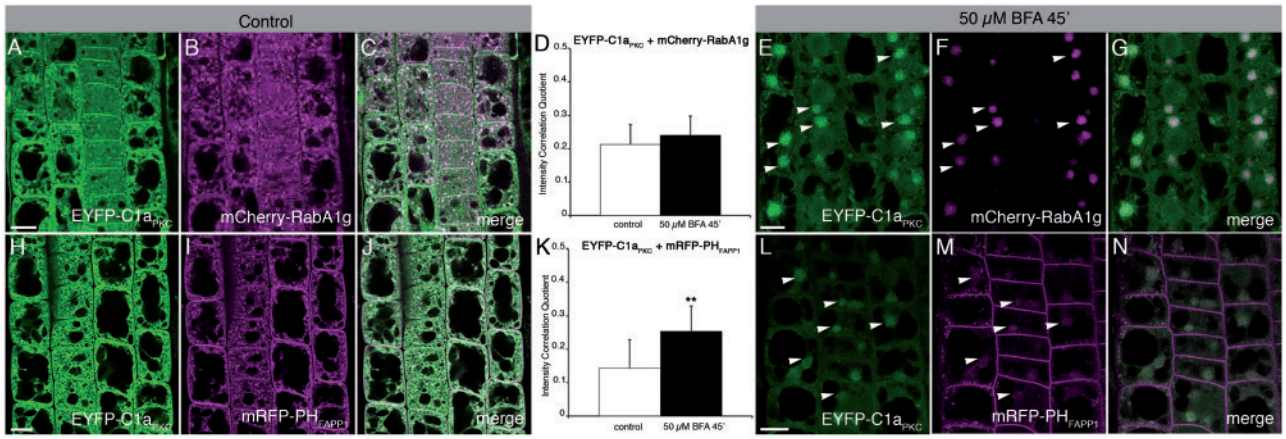

Fig. 4 YFP–C1a$_{PKC}$ detects DAG at the TGN. Confocal fluorescence images of Arabidopsis seedlings co-expressing 35S::EYFP–C1a$_{PKC}$ and UBQ10::mCherry–RabA1g (A–C and E–G) or 35S::EYFP–C1a$_{PKC}$ and 35S::mRFP–PH$_{FAPP1}$ (H–J and L–N). EYFP–C1a$_{PKC}$ shows partial co-localization with both the TGN marker mCherry–RabA1g (D) and the PI4P biosensor mRFP–PH$_{FAPP1}$ (K). (E–G and L–M) The effect of BFA treatment (50 μM 45 min) on the subcellular localization of the marker used. Whereas both EYFP–C1a$_{PKC}$ and mCherry–RabA1g show strong accumulation in BFA compartments, mRFP–PH$_{FAPP1}$ only shows weak accumulation. (D and K) Quantification of co-localization based on the images including those shown in (A–C and E–G) and (H–J and L–N), measured as intensity correlation of pixels (ICQ), with a value of zero indicating no co-localization, and a value of 0.5 indicating complete overlap. Note that BFA treatment results in a significant increase in overlap between EYFP–C1a$_{PKC}$ and mRFP–PH$_{FAPP1}$. Asterisks indicate significant differences (**$P < < 0.5 \times E^{-7}$) by Student *t*-test. EYFP is shown in green and mRFP or mCherry is shown in magenta. Scale bars = 10 μm.

S1, S2). Mutating the amino acid residue critical for lipid binding rendered the fusion protein cytosolic and insensitive to PMA treatment in Arabidopsis seedlings (**Supplementary Fig. S6**). Together these data confirm that the biosensor is bona fide and detects DAG. The predominant cytosolic localization of the fusion protein indicates that the DAG level in the cytoplasmic leaflets of most plant membranes is relatively low, which is actually similar to animal cells. Some DAG could be in the nucleus (Albi et al. 2008, Dieck et al. 2012a, Dieck et al. 2012b), although we did not observe any clear relocalization of YFP–C1a$_{PKC}$ into the nucleus, while PMA treatment diminished this nuclear fluorescence, suggesting that the sensor can freely diffuse between the cytosol and nucleus (**Supplementary Fig. S1**).

We did not observe labeling of ER, mitochondria or plastids, which are organelles known to contain DAG (Dörmann and Benning 2002, Dong et al. 2012, Muthan et al. 2013). While this appears to be contradictory at first, one should realize that YFP–C1a$_{PKC}$ is localized in the cytosol so can only detect DAG facing the cytoplasmic leaflet of membranes. Since the biosensor is not detecting any ER-, mitochondrial- or plastid-resident DAG, our results suggest that these DAG pools are located at the luminal side of these organelles. The latter has recently been confirmed for plastids (Muthan et al. 2013). Alternatively, DAG could be bound to proteins with a higher affinity than the biosensor, or, due to its flip–flop behavior, may not be available long enough for the sensor to bind it. Nonetheless, YFP–C1a$_{PKC}$ did detect some transient accumulation of DAG at the plasma membrane of epidermal cells in the transition zone of Arabidopsis roots, and by employing a biosensor with increased avidity, EYFP–2 × C1a$_{PKC}$, this became more evident. The fact that the latter biosensor also did not reveal any signal at the ER, mitochondrion or plastid confirms that these pools are inaccessible to the biosensor. A recent study in mammalian cells, using a similar approach, did not detect DAG at the ER either, but found a novel motile organelle (Kim et al. 2015).

The observed transient accumulation of YFP–2 × C1a$_{PKC}$ in the root epidermis might reflect a specific role for the phosphoinositide signaling circuit during the transition of epidermal cells into differentiation. This is supported by the recently observed bipolar localization of PI4P, PI(4,5)P2 and the PIP 5-kinases, AtPIP5K1 and AtPIP5K2, which was shown to be required for polarity and patterning (Ischebeck et al. 2013, Tejos et al. 2014). The fact that YFP–C1a$_{PKC}$ also detected DAG at the TGN, cell plate and growing root hairs points to differential behavior of DAG in different membranes, which may reflect distinct functions (see below).

An important feature of YFP–C1a$_{PKC}$ and YFP–2 × C1a$_{PKC}$ is that they apparently do not outcompete endogenous DAG binding/metabolism, permitting their use to monitor DAG in living plant cells. Targeting of the biosensor to specific organelles may even be used to investigate intraorganelle DAG pools, although the resolution of the confocal microscope may be too limited to discriminate between soluble and membrane-bound YFP–C1a$_{PKC}$. Nonetheless, immunogold labeling and electron microscopy could extend the use of this DAG sensor.

The presence of DAG at TGN membranes has also been reported for mammalian cells, where DAG locally activates protein kinase D (PKD) to mediate protein release from the TGN via its C1 domain (Maeda et al. 2001, Baron and Malhotra 2002, Yeaman et al. 2004). Whether similar mechanisms exist in plants is unknown. At least this will not involve PKC or PKD since plant genomes lack homologs of these kinases (Testerink

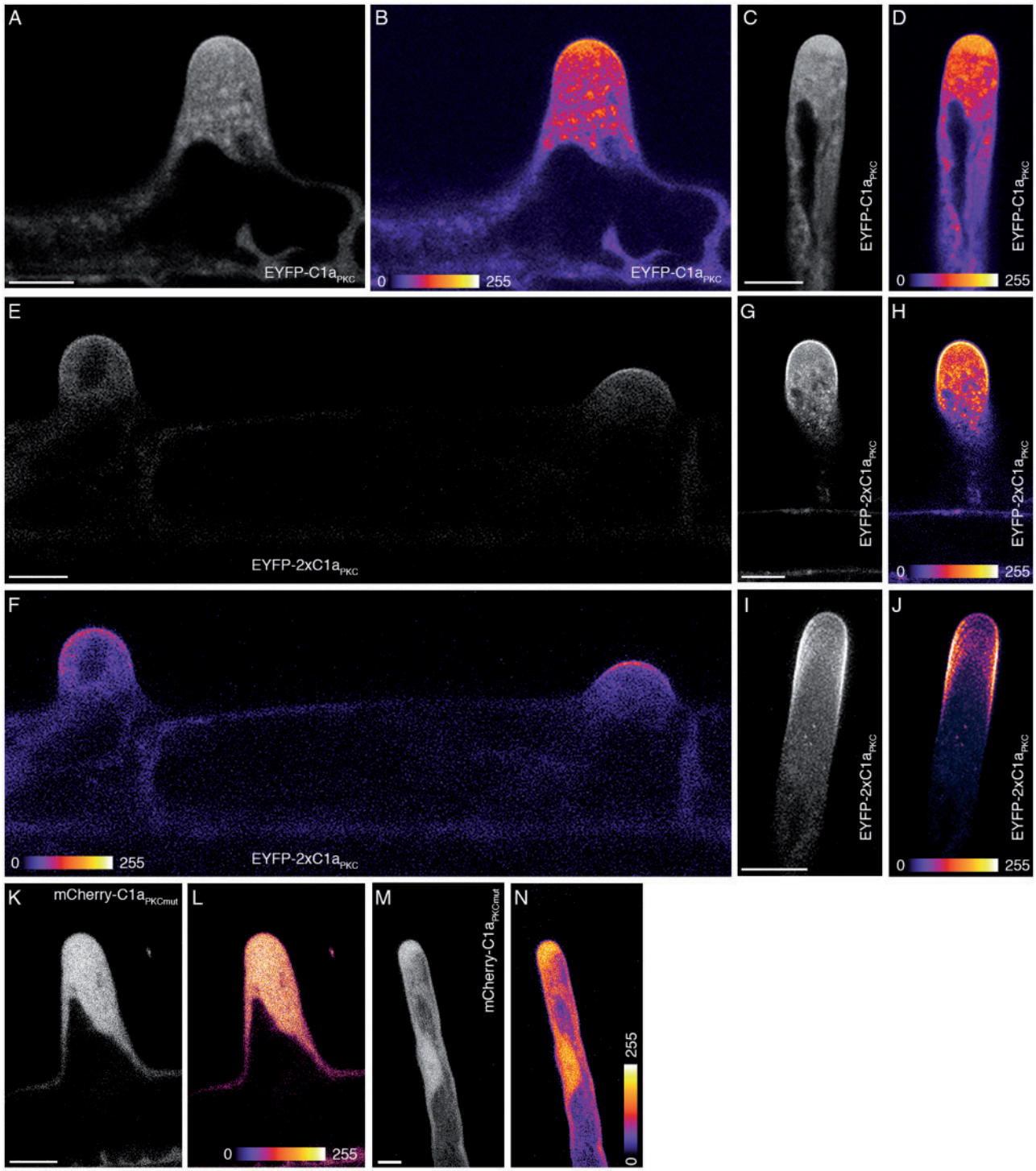

Fig. 5 Polar localization of YFP–C1a$_{PKC}$ in growing root hairs. Confocal fluorescence images of root hairs of 5-day-old Arabidopsis seedlings expressing 35S::YFP–C1a$_{PKC}$ (A–D) or UBQ10::EYFP–2 × C1a$_{PKC}$ (E–J). (A, B) Young bulging root hair, (C, D) root hair undergoing tip growth, (E, F) two bulging root hairs and emerging root hair. (G, H) Plasma membrane labeling of EYFP–2 × C1a$_{PKC}$ at the apex as well as labeling of punctated structures. (I, J) Root hair undergoing tip growth showing accumulation of YFP–2 × C1a$_{PKC}$ fluorescence in the shanks of the root hair apex (see also **Supplementary Movie S3**). (K–N) Growing root hairs of plants expressing UBQ10::mCherry–C1a$_{PKCmut}$ showing cytosolic localization and absence of a tip-focused gradient. YFP and mCherry are shown in gray (A, C, E, G, I, K, M) or in a false color gradient to enhance signal intensity ranging from 0 to 255 gray values. Scale bar = 10 μm.

and Munnik 2011). They do, however, encode proteins containing a C1 domain (or C1-like), but it is unknown whether these domains can actually bind DAG. While direct evidence for a signaling role for DAG is lacking in plants, there is substantial evidence that PLC-generated DAG is rapidly phosphorylated to PA (Munnik et al. 2000, Arisz et al. 2009), and that it is the latter that functions as a lipid second messenger, recruiting and activating signaling proteins, including protein kinases (Testerink

and Munnik 2005, Mishra et al. 2006, Zhang et al. 2009, Testerink and Munnik 2011, Gasulla et al. 2016, Hou et al. 2016). PA can also be generated by phospholipase D but, pools can be distinguished through a transphosphatidylation and differential $^{32}P_i$ labeling protocol (Arisz et al. 2009, Arisz and Munnik 2013).

The current data may also have implications for the PLC signaling pathway in plants. As mentioned earlier, higher plants exhibit extremely low PI(4,5)P_2 levels, and one of the explanations for this could be a high intrinsic PLC activity at the plasma membrane, constantly hydrolyzing PI(4,5)P_2 (van Leeuwen et al. 2007). If so, one would expect then to find a steady-state localization of the DAG at the plasma membrane, and this is not what we typically observed (**Fig. 1**; **Supplementary Fig. 4**). If, however, this DAG would be instantly converted into PA by DGK, then this could explain the lack of correlation. While PLC and DGK activity are indeed enriched at the plasma membrane of various plant species (Munnik et al. 1998a), it remains unknown whether this occurs in a complex.

Ultimately, the development of a bona fide PA biosensor will provide further insight into the connection between DAG and PA, in localization and kinetics. For pollen, a PA biosensor has recently been reported. It consists of a fluorescent protein fusion with the PA-binding domain of yeast protein, Spo20, which was transiently expressed in pollen tubes (Potocky et al. 2014). We have stably expressed the same biosensor in tobacco BY-2 cells and Arabidopsis plants, but, in contrast to pollen, no typical membrane localization was found, even when cells or seedlings were challenged with cold, heat or salt stress (R. van Wijk, J.E.M. Vermeer and T. Munnik, unpublished), which are known to boost PA levels within minutes (Munnik et al. 2000, Bargmann et al. 2009a, Bargmann et al. 2009b, Mishkind et al. 2009, Arisz et al. 2013). Moreover, a recent lipid binding study on the Spo20 domain suggests that it interacts non-specifically with anionic lipids, including PA, PS and PI(4,5)P_2 (Horchani et al. 2014). Hence, future research and clarity will be required to image PA conclusively in plant cells.

Role for DAG during plant cytokinesis

In both plant systems, we found that YFP–$C1a_{PKC}$ and YFP–$2 \times C1a_{PKC}$ accumulated at forming cell plates (**Figs. 2**, 3F; **Supplementary Movie S1**). Co-labeling with the endocytic tracer FM4-64 revealed that this dye labeled the cell plate just slightly before (**Fig. 2**; **Supplementary Movie S1**), resembling a pattern that we observed earlier for the PI4P biosensor, YFP–PH_{FAPP1} (Vermeer et al. 2009). The latter clearly labels the plasma membrane and Golgi membranes (Vermeer et al. 2009). The fact that both PI4P and DAG are present on Golgi membranes and on the forming cell plate may indicate that these lipids are mutually involved in membrane traffic from the Golgi to the cell plate. Theoretically, PLC can also hydrolyze PI4P to generate DAG (Munnik 2014). Another explanation could be a localized PLC hydrolysis of PI(4,5)P_2. This would fit with our earlier observation that PI(4,5)P_2 does not seem to accumulate at the cell plate, but only transiently at the leading edges, prior to fusion with the parental plasma membrane (van Leeuwen et al. 2007). Alternatively, since the building of a cell plate requires the synthesis of a complete new membrane, another explanation could be that the observed accumulation represents net synthesis of PC and PE via the Kennedy pathway (Gibellini and Smith 2010). However, this DAG synthesis is believed to occur within the ER lumen, a compartment that is normally not accessible to our biosensor. Another possibility is that the accumulation of DAG at the cell plate mirrors the activity of an NPC or a specific inositol phosphorylceramide synthase (Inositol Phosphorylceramide Synthase(IPC); the latter produces DAG as a side product at the cost of PIP and ceramide) (Denny et al. 2006, Fakas et al. 2011, Arisz et al. 2013, Nakamura 2014). Such coupled production and metabolism of DAG might explain the relative stable cell plate signal of YFP–$C1a_{PKC}$ and could also explain why we do not see any labeling of the parental plasma membrane, as no additional (structural) lipids would be required. Subcellular localization studies and knockout mutants of PLC, NPC, IPC and other enzymes involved in DAG metabolism would be helpful to answer some of these new questions.

A possible role for DAG in tip growth?

Earlier, we and others used lipid biosensors for PI4P (EYFP–PH_{FAPP1}) and PI(4,5)P_2 (EYFP–$PH_{PLC}\delta_1$) to visualize gradients of PI4P and PI(4,5)P_2 in the plasma membrane of growing root hairs and pollen tubes, and this has been suggested to reflect their role in regulating tip growth (Kost et al. 1999, Vincent et al. 2005, Dowd et al. 2006, Helling et al. 2006, van Leeuwen et al. 2007, Vermeer et al. 2009). This idea has been substantiated by characterizing several enzymes that are involved in regulating cellular levels of PI4P and PI(4,5)P_2 (Dowd et al. 2006, Preuss et al. 2006, Helling et al. 2006, Ischebeck et al. 2008, Kusano et al. 2008, Sousa et al. 2008, Stenzel et al. 2008, Thole et al. 2008, Camacho et al. 2009, Wada et al. 2015). While these studies clearly show that PPIs are important players in an intricate trafficking mechanism that regulates tip growth (Kost 2008, Thole and Nielsen 2008, Ischebeck et al. 2010, Munnik and Nielsen 2011), the role of PLC in controlling the balance between PPIs and DAG is still unclear (Munnik and Nielsen 2011, Munnik 2014). PLC has been reported to participate in the regulation of pollen tube growth, but this was only based on the transient overexpression of active and inactive PLC variants (Dowd et al. 2006, Helling et al. 2006, Zhao et al. 2010). Moreover, these studies only considered PI(4,5)P_2 as a PLC substrate, while PI4P could also be a substrate (Munnik and Vermeer 2010, Munnik and Nielsen 2011, Munnik 2014), and this would explain the same accumulation of DAG at the plasma membrane.

In bulging root hairs, YFP–$C1a_{PKC}$ labeled the plasma membrane at the apex, whereas in rapidly growing root hairs, we also observed the labeling of a TGN compartment positioned under the tip, and weak labeling of the plasma membrane at the shanks just below the tip (**Fig. 5**). The latter localization at the shanks of the root hair tip became very clear in growing root hairs expressing YFP–$2 \times C1a_{PKC}$ (**Fig. 5**). The localization of YFP–$C1a_{PKC}$ and YFP–$2 \times C1a_{PKC}$ is in agreement with the observed accumulation of NtPLC3 in growing pollen tubes, although Helling et al. (2006) did not observe clear labeling of a

TGN compartment using the same C1a-based sensor (Helling et al. 2006). Besides the difference in experimental design (stable vs. transient overexpression), and although tip growth of pollen tubes and root hairs are very much alike, there may also be some differences.

To dissect the possible role(s) of DAG in polar growth, a further in-depth characterization of Arabidopsis PLC and DGK enzymes will be required. Combined with forward (chemical) genetic screens, and based on the relocalization of single and double DAG biosensors, this is likely to provide new insights into plant lipid signaling and metabolism.

Materials and Methods

Constructs

All constructs were produced using standard molecular biological procedures. To generate pEYFP–C1a$_{PKC}$, the C1a domain (amino acids 26–86) from rat PKCγ was amplified from plasmid pC1a$_{PKC}$–GFP using the primers Bgl2_C1a-fw ga**agatct**aggcagaaggtggtccac and EcoRI_C1a-rv cg**gaattc**ttacttgtacagctcgtc, and ligated to pEYFP-C1. Next, the EYFP–C1a$_{PKC}$ fragment was cloned into pMONd35S (Vermeer et al. 2004) using *Xba*I and *Eco*RI. For plant transformation, the 35S-EYFP–C1a$_{PKC}$-Tnos or the 35S-mRFP–PH$_{FAPP1}$-Tnos fragments were transferred to pGreen179 using *Not*I. To generate pUBQ10::EYFP-C1a$_{PKC}$ and pUBQ10::EYFP-2 × C1a$_{PKC}$, we first cloned C1a$_{PKC}$ and 2 × C1a$_{PKC}$ in pUNI51. pUNI51-C1a$_{PKC}$ and pUNI51-2 × C1a$_{PKC}$ were recombined into pNIGEL07 using Cre/Lox recombination as described (Geldner et al. 2009). To generate pGreen179-UBQ10::mCherry-C1a$_{PKCP46G}$, the C1a$_{PKC}$ domain was PCR amplified and cloned in-frame with mCherry using the primers C1a_EcoRIfw gg**gaattc**agcggaaggcagaaggtggtccac and C1a_XbaIrv gc**tctaga**ttaggtggcgaccggtgg. The P46G point mutation was introduced with site-directed mutagenesis using the primers C1a_P > Gfw cgtttcttcaagcagGGAaccttctgcagtcactg and C1a_P > Grv cagtgactgcagaaggtTCCctgcttgaagaaacg. pGreen179-35S-mRFP-PH$_{FAPP1}$ has been described before (Vermeer et al. 2009).

Plant material

Cowpea protoplast were isolated and transfected as described before (Vermeer et al. 2006). Tobacco BY-2 cells were transformed and subcultured as described previously (Vermeer et al. 2006). Arabidopsis plants were transformed using floral dip transformation (Clough and Bent 1998). Homozygous T_3 plants were used for further analysis. Seeds were germinated on 0.5 × Murashige and Skoog (MS) containing 1% sucrose and 1% agar. Arabidopsis plants expressing free EYFP or mCherry–RabA1g were from the Wave Line collection (Geldner et al. 2009). F_1 seedlings were used for co-localization experiments.

Confocal microscopy and image analysis

BY-2 cells (4–5 d old) or protoplasts were mounted in eight-chambered cover slides (Nalge Nunc International; www.nuncbrand.com). Five- to seven-day-old seedlings were mounted on cover slides or in Nunc chambers and covered by a cover glass or a block of agar, respectively. Fluorescence microscopy was performed using a Zeiss LSM 510, 710, Leica SP5 or SP8 confocal laser scanning microscope implemented on an inverted microscope. Excitation was provided at 488 nm or 561 nm for GFP/FM4-64 and mCherry, respectively. For YFP fluorescence, an excitation/emission combination of 488 nm and 505–550 nm detection was used. For YFP/FM4-64 fluorescence, an excitation/emission combination of 488 nm/505–550 nm for YFP was combined with long pass 650 nm for FM4-64. For YFP/mRFP/mCherry dual scanning, we used the excitation/emission combinations of 488 nm/505–550 nm for YFP and 561 nm/600–650 nm for red fluorescent protein (RFP)/mCherry. Cross-talk-free images were acquired by operating the microscope in the sequential-aquisition mode. A Zeiss × 40 water-immersion objective, Zeiss × 40 oil objective, Zeiss × 63 water objective or a Leica × 63 water objective were used. Images were captured and analyzed using ZEISS LSM510 software (version 3.2 SP3), Zeiss ZEN 2012 and LAS-X and processed using FIJI with the macbiophotonics bundle (www.macbiophotonics.ca/imagej/installing_imagej.htm). Intensity correlation analysis delivers a coefficient that ranges between 0.5 and zero for complete co-localization or non-co-localization, respectively. We found some advantages of intensity correlation analysis over other methods, in that it takes into account the relative intensities of co-localizing pixels, and can be performed without thresholding. For the analysis of YFP–C1a$_{PKC}$-positive structures, regions of interest (ROIs) of entire cells, excluding the plasma membrane, were examined. At least 20 different ROIs were analyzed. Error bars indicate the SD of the mean.

Western blot analysis

Roots of 11-day old seedlings were ground in liquid nitrogen and proteins were extracted using 2 × (w/v) protein extraction buffer [0.5% (v/v) NP-40, 75 mM NaCl, 100 mM Tris–HCl pH 8.0, 1% (w/v) polyvinylpolypyrrolidone (PVPP), 100 mM dithiothreitol (DTT), 1 mM phenylmethylsulfonyl fluoride (PMSF), 10 mM EDTA (pH 8.0) and complete, EDTA-free Protease Inhibitor Cocktail (Roche)]. The total protein concentration in the supernatant (30 min, 18,000 × *g*, 4°C) was determined by nanodrop (ThermoFisher). A 60 μg aliquot of total protein per sample was separated on a 12% SDS–polyacrylamide gel and blotted on polyvinylidene fluoride (PVDF; Immobilon P, Millipore). The Western blot analysis was performed using a polyclonal anti-GFP rabbit serum (A-6455, ThermoFisher) and a second antibody, goat anti-rabbit peroxidase (131460, Pierce).

Supplementary data

Supplementary data are available at PCP online.

Funding

This work was supported by the Howard Hughes Medical Institute and National Science Foundation [IOS-0649389 to N.G. and J.C.]; the European Commission [Marie-Curie IEF

grant 253729-CASDEV to J.E.M.V. and COST FA0605 to T.M]; the Netherlands Organization for Scientific Research [NWO 864.13.008 to J.E.M.V. and 867.15.020 to T.M.]; and the Swiss National Science Foundation [PP00P3_157524 to J.E.M.V.].

Acknowledgments

We thank Dr. Tobias Meyer (Stanford University Medical Center, CA, USA) for kindly providing us with pC1a-GFP, and Valerie Denervaud-Tendon (University of Lausanne, Switzerland) for technical assistance with the WAVE lines.

Disclosures

The authors have no conflicts of interest to declare.

References

Albert, A.P. (2011) Gating mechanisms of canonical transient receptor potential channel proteins: role of phosphoinositols and diacylglycerol. *Adv. Exp. Med. Biol.* 704: 391–411.

Albi, E., Cataldi, S., Rossi, G., Viola Magni, M., Toller, M., Casani, S., et al. (2008) The nuclear ceramide/diacylglycerol balance depends on the physiological state of thyroid cells and changes during UV-C radiation-induced apoptosis. *Arch. Biochem. Biophys.* 478: 52–58.

Arisz, S.A. and Munnik, T. (2013) Distinguishing phosphatidic acid pools from de novo synthesis, PLD, and DGK. *Methods Molec. Biol.* 1009: 55–62.

Arisz, S.A., Testerink, C. and Munnik, T. (2009) Plant PA signaling via diacylglycerol kinase. *Biochim. Biophys. Acta* 1791: 869–875.

Arisz, S.A., van Himbergen, J.A., Musgrave, A., van den Ende, H. and Munnik, T. (2000) Polar glycerolipids of Chlamydomonas moewusii. *Phytochemistry* 53: 265–270.

Arisz, S.A., van Wijk, R., Roels, W., Zhu, J.K., Haring, M.A. and Munnik, T. (2013) Rapid phosphatidic acid accumulation in response to low temperature stress in Arabidopsis is generated through diacylglycerol kinase. *Front. Plant Sci.* 4: 1.

Bargmann, B.O., Laxalt, A.M., ter Riet, B., Testerink, C., Merquiol, E., Mosblech, A., et al. (2009a) Reassessing the role of phospholipase D in the Arabidopsis wounding response. *Plant Cell Environ.* 32: 837–850.

Bargmann, B.O., Laxalt, A.M., ter Riet, B., van Schooten, B., Merquiol, E., Testerink, C., et al. (2009b) Multiple PLDs required for high salinity and water deficit tolerance in plants. *Plant Cell Physiol.* 50: 78–89.

Baron, C.L. and Malhotra, V. (2002) Role of diacylglycerol in PKD recruitment to the TGN and protein transport to the plasma membrane. *Science* 295: 325–328.

Bates, P.D., Durrett, T.P., Ohlrogge, J.B. and Pollard, M. (2009) Analysis of acyl fluxes through multiple pathways of triacylglycerol synthesis in developing soybean embryos. *Plant Physiol.* 150: 55–72.

Benning, C. (2009) Mechanisms of lipid transport involved in organelle biogenesis in plant cells. *Annu. Rev. Cell Dev. Biol.* 25: 71–91.

Boss, W.F. and Im, Y.J. (2012) Phosphoinositide signaling. *Annu. Rev. Plant Biol.* 63: 409–429.

Bossard, C., Bresson, D., Polishchuk, R.S. and Malhotra, V. (2007) Dimeric PKD regulates membrane fission to form transport carriers at the TGN. *J. Cell Biol.* 179: 1123–1131.

Bruce, B.D. (1998) The role of lipids in plastid protein transport. *Plant Mol. Biol.* 38: 223–246.

Camacho, L., Smertenko, A.P., Perez-Gomez, J., Hussey, P.J. and Moore, I. (2009) Arabidopsis Rab-E GTPases exhibit a novel interaction with a plasma-membrane phosphatidylinositol-4-phosphate 5-kinase. *J. Cell Sci.* 122: 4383–4392.

Clough, S.J. and Bent, A.F. (1998) Floral dip: a simplified method for Agrobacterium-mediated transformation of Arabidopsis thaliana. *Plant J.* 16: 735–743.

Denny, P.W., Shams-Eldin, H., Price, H.P., Smith, D.F. and Schwarz, R.T. (2006) The protozoan inositol phosphorylceramide synthase: a novel drug target that defines a new class of sphingolipid synthase. *J. Biol. Chem.* 281: 28200–28209.

Desai, M., Rangarajan, P., Donahue, J.L., Williams, S.P., Land, E.S., Mandal, M.K., et al. (2014) Two inositol hexakisphosphate kinases drive inositol pyrophosphate synthesis in plants. *Plant J.* 80: 642–653.

Dieck, C.B., Boss, W.F. and Perera, I.Y. (2012a) A role for phosphoinositides in regulating plant nuclear functions. *Front. Plant Sci.* 3: 50.

Dieck, C.B., Wood, A., Brglez, I., Rojas-Pierce, M. and Boss, W.F. (2012b) Increasing phosphatidylinositol (4,5) bisphosphate biosynthesis affects plant nuclear lipids and nuclear functions. *Plant Physiol. Biochem.* 57: 32–44.

Dong, W., Lv, H., Xia, G. and Wang, M. (2012) Does diacylglycerol serve as a signaling molecule in plants? *Plant Signal. Behav.* 7: 472–475.

Dörmann, P. and Benning, C. (2002) Galactolipids rule in seed plants. *Trends Plant Sci.* 7: 112–118.

Dowd, P.E., Coursol, S., Skirpan, A.L., Kao, T.H. and Gilroy, S. (2006) Petunia phospholipase c1 is involved in pollen tube growth. *Plant Cell* 18: 1438–1453.

Dowd, P.E. and Gilroy, S. (2010) The emerging roles of phospholipase c in plant growth and development. *In* Lipid Signaling in Plants. Edited by Munnik, T. pp. 23–38. Springer Verlag, Berlin.

Fakas, S., Konstantinou, C. and Carman, G.M. (2011) DGK1-encoded diacylglycerol kinase activity is required for phospholipid synthesis during growth resumption from stationary phase in *Saccharomyces cerevisiae*. *J. Biol. Chem.* 286: 1464–1474.

Gasulla, F., Barreno, E., Parages, M.L., Camara, J., Jimenez, C., Dormann, P., et al. (2016) The role of phospholipase D and MAPK signaling cascades in the adaption of lichen microalgae to desiccation: changes in membrane lipids and phosphoproteome. *Plant Cell Physiol.* 57: 1908–1920.

Gaude, N., Brehelin, C., Tischendorf, G., Kessler, F. and Dörmann, P. (2007) Nitrogen deficiency in Arabidopsis affects galactolipid composition and gene expression and results in accumulation of fatty acid phytyl esters. *Plant J.y* 49: 729–739.

Gaude, N., Nakamura, Y., Scheible, W.R., Ohta, H. and Dörmann, P. (2008) Phospholipase C5 (NPC5) is involved in galactolipid accumulation during phosphate limitation in leaves of Arabidopsis. *Plant J.* 56: 28–39.

Geldner, N., Anders, N., Wolters, H., Keicher, J., Kornberger, W., Muller, P., et al. (2003) The Arabidopsis GNOM ARF-GEF mediates endosomal recycling, auxin transport, and auxin-dependent plant growth. *Cell* 112: 219–230.

Geldner, N., Denervaud-Tendon, V., Hyman, D.L., Mayer, U., Stierhof, Y.D. and Chory, J. (2009) Rapid, combinatorial analysis of membrane compartments in intact plants with a multicolor marker set. *Plant J.* 59: 169–178.

Gibellini, F. and Smith, T.K. (2010) The Kennedy pathway—de novo synthesis of phosphatidylethanolamine and phosphatidylcholine. *IUBMB Life* 62: 414–428.

Gillaspy, G.E. (2013) The role of phosphoinositides and inositol phosphates in plant cell signaling. *Adv. Exp. Med. Biol.* 991: 141–157.

Hammond, G.R. and Balla, T. (2015) Polyphosphoinositide binding domains: key to inositol lipid biology. *Biochim. Biophys. Acta.* 1851: 746–758.

Heilmann, I. (2008a) Tails wagging the dogs: on phosphoinositides and their fatty acyl moieties. *Plant Signal. Behav.* 3: 768–771.

Heilmann, I. (2008b) Towards understanding the function of stress-inducible PtdIns(4,5)P(2) in plants. *Commun. Integr. Biol.* 1: 204–206.

Heilmann, I. (2016) Phosphoinositide signaling in plant development. *Development* 143: 2044–2055.

Heilmann, M. and Heilmann, I. (2015) Plant phosphoinositides—complex networks controlling growth and adaptation. *Biochim. Biophys. Acta* 1851: 759–769.

Helling, D., Possart, A., Cottier, S., Klahre, U. and Kost, B. (2006) Pollen tube tip growth depends on plasma membrane polarization mediated by tobacco PLC3 activity and endocytic membrane recycling. *Plant Cell* 18: 3519–3534.

Horchani, H., de Saint-Jean, M., Barelli, H. and Antonny, B. (2014) Interaction of the Spo20 membrane-sensor motif with phosphatidic acid and other anionic lipids, and influence of the membrane environment. *PLoS One* 9: e113484.

Hou, Q., Ufer, G. and Bartels, D. (2016) Lipid signalling in plant responses to abiotic stress. *Plant Cell Environ.* 39: 1029–1048.

Ischebeck, T., Seiler, S. and Heilmann, I. (2010) At the poles across kingdoms: phosphoinositides and polar tip growth. *Protoplasma* 240: 13–31.

Ischebeck, T., Stenzel, I. and Heilmann, I. (2008) Type B phosphatidylinositol-4-phosphate 5-kinases mediate Arabidopsis and Nicotiana tabacum pollen tube growth by regulating apical pectin secretion. *Plant Cell* 20: 3312–3330.

Ischebeck, T., Werner, S., Krishnamoorthy, P., Lerche, J., Meijon, M., Stenzel, I., et al. (2013) Phosphatidylinositol 4,5-bisphosphate influences PIN polarization by controlling clathrin-mediated membrane trafficking in Arabidopsis. *Plant Cell* 25: 4894–4911.

Kang, B.H., Nielsen, E., Preuss, M.L., Mastronarde, D. and Staehelin, L.A. (2011) Electron tomography of RabA4b- and PI-4Kbeta1-labeled trans Golgi network compartments in Arabidopsis. *Traffic* 12: 313–329.

Kaup, M.T., Froese, C.D. and Thompson, J.E. (2002) A role for diacylglycerol acyltransferase during leaf senescence. *Plant Physiol.* 129: 1616–1626.

Kim, Y.J., Guzman-Hernandez, M.L. and Balla, T. (2011) A highly dynamic ER-derived phosphatidylinositol-synthesizing organelle supplies phosphoinositides to cellular membranes. *Dev. Cell* 21: 813–824.

Kim, Y.J., Guzman-Hernandez, M.L., Wisniewski, E. and Balla, T. (2015) Phosphatidylinositol–phosphatidic acid exchange by Nir2 at ER–PM contact sites maintains phosphoinositide signaling competence. *Dev. Cell* 33: 549–561.

Kocourkova, D., Krckova, Z., Pejchar, P., Veselkova, S., Valentova, O., Wimalasekera, R., et al. (2011) The phosphatidylcholine-hydrolysing phospholipase C NPC4 plays a role in response of Arabidopsis roots to salt stress. *J. Exp. Bot.* 62: 3753–3763.

Kost, B. (2008) Spatial control of Rho (Rac–Rop) signaling in tip-growing plant cells. *Trends Cell Biol.* 18: 119–127.

Kost, B., Lemichez, E., Spielhofer, P., Hong, Y., Tolias, K., Carpenter, C., et al. (1999) Rac homologues and compartmentalized phosphatidylinositol 4, 5-bisphosphate act in a common pathway to regulate polar pollen tube growth. *J. Cell Biol.* 145: 317–330.

Kusano, H., Testerink, C., Vermeer, J.E., Tsuge, T., Shimada, H., Oka, A., et al. (2008) The Arabidopsis phosphatidylinositol phosphate 5-kinase PIP5K3 is a key regulator of root hair tip growth. *Plant Cell* 20(2): 367–80.

Maeda, Y., Beznoussenko, G.V., Van Lint, J., Mironov, A.A. and Malhotra, V. (2001) Recruitment of protein kinase D to the trans-Golgi network via the first cysteine-rich domain. *EMBO J.* 20: 5982–5990.

Meijer, H.J. and Munnik, T. (2003) Phospholipid-based signaling in plants. *Annu. Rev. Plant Biol.* 54: 265–306.

Mishkind, M., Vermeer, J.E., Darwish, E. and Munnik, T. (2009) Heat stress activates phospholipase D and triggers PIP accumulation at the plasma membrane and nucleus. *Plant J.* 60: 10–21.

Mishra, G., Zhang, W., Deng, F., Zhao, J. and Wang, X. (2006) A bifurcating pathway directs abscisic acid effects on stomatal closure and opening in Arabidopsis. *Science* 312: 264–266.

Mueller-Roeber, B. and Pical, C. (2002) Inositol phospholipid metabolism in Arabidopsis. Characterized and putative isoforms of inositol phospholipid kinase and phosphoinositide-specific phospholipase C. *Plant Physiol.* 130: 22–46.

Munnik, T. (2014) PI–PLC: phosphoinositide–phospholipase C in plant signaling. *In* Phospholipases in Plant Signaling. Edited by Wang, X. pp. 27–54. Springer-Verlag, Berlin.

Munnik, T., Irvine, R.F. and Musgrave, A. (1998a) Phospholipid signalling in plants. *Biochim. Biophys. Acta* 1389: 222–272.

Munnik, T., Meijer, H.J., Ter Riet, B., Hirt, H., Frank, W., Bartels, D., et al. (2000) Hyperosmotic stress stimulates phospholipase D activity and elevates the levels of phosphatidic acid and diacylglycerol pyrophosphate. *Plant J.* 22: 147–154.

Munnik, T., Musgrave, A. and de Vrije, T. (1994) Rapid turnover of polyphosphoinositides in carnation flower petals. *Planta* 193: 89–98.

Munnik, T. and Nielsen, E. (2011) Green light for polyphosphoinositide signals in plants. *Curr. Opin. Plant Biol.* 14: 489–497.

Munnik, T. and Testerink, C. (2009) Plant phospholipid signaling: 'in a nutshell'. *J. Lipid Res.* 50 Suppl: S260–S265.

Munnik, T., van Himbergen, J.A.J., Ter Riet, B., Braun, F., Irvine, R.F., van den Ende, H., et al. (1998b) Detailed analysis of the turnover of polyphosphoinositides and phosphatidic acid upon activation of phospholipases C and D in *Chlamydomonas* cells treated with non-permeabilizing concentrations of mastoparan. *Planta* 207: 133–145.

Munnik, T. and Vermeer, J.E. (2010) Osmotic stress-induced phosphoinositide and inositol phosphate signalling in plants. *Plant Cell Environ.* 33: 655–669.

Muthan, B., Roston, R.L., Froehlich, J.E. and Benning, C. (2013) Probing Arabidopsis chloroplast diacylglycerol pools by selectively targeting bacterial diacylglycerol kinase to suborganellar membranes. *Plant Physiol.* 163: 61–74.

Nakamura, Y. (2014) NPC: nonspecific phospholipase Cs in plant functions. *In* Phospholipases in Plant Signaling. Edited by Wang, X. pp. 55–67. Springer-Verlag, Berlin.

Nakamura, Y., Awai, K., Masuda, T., Yoshioka, Y., Takamiya, K. and Ohta, H. (2005) A novel phosphatidylcholine-hydrolyzing phospholipase C induced by phosphate starvation in Arabidopsis. *J. Biol. Chem.* 280: 7469–7476.

Nakamura, Y., Koizumi, R., Shui, G., Shimojima, M., Wenk, M.R., Ito, T., et al. (2009) Arabidopsis lipins mediate eukaryotic pathway of lipid metabolism and cope critically with phosphate starvation. *Proc. Natl. Acad. Sci. USA* 106: 20978–20983.

Oancea, E. and Meyer, T. (1998) Protein kinase C as a molecular machine for decoding calcium and diacylglycerol signals. *Cell* 95: 307–318.

Oancea, E., Teruel, M.N., Quest, A.F. and Meyer, T. (1998) Green fluorescent protein (GFP)-tagged cysteine-rich domains from protein kinase C as fluorescent indicators for diacylglycerol signaling in living cells. *J. Cell Biol.* 140: 485–498.

Peters, C., Kim, S.C., Devaiah, S., Li, M. and Wang, X. (2014) Non-specific phospholipase C5 and diacylglycerol promote lateral root development under mild salt stress in Arabidopsis. *Plant Cell Environ.* 37: 2002–2013.

Peters, C., Li, M., Narasimhan, R., Roth, M., Welti, R. and Wang, X. (2010) Nonspecific phospholipase C NPC4 promotes responses to abscisic acid and tolerance to hyperosmotic stress in Arabidopsis. *Plant Cell* 22: 2642–2659.

Pokotylo, I., Kolesnikov, Y., Kravets, V., Zachowski, A. and Ruelland, E. (2014) Plant phosphoinositide-dependent phospholipases C: variations around a canonical theme. *Biochimie* 96: 144–157.

Potocky, M., Pleskot, R., Pejchar, P., Vitale, N., Kost, B. and Zarsky, V. (2014) Live-cell imaging of phosphatidic acid dynamics in pollen tubes visualized by Spo20p-derived biosensor. *New Phytol.* 203: 483–494.

Preuss, M.L., Schmitz, A.J., Thole, J.M., Bonner, H.K., Otegui, M.S. and Nielsen, E. (2006) A role for the RabA4b effector protein PI-4Kbeta1 in polarized expansion of root hair cells in Arabidopsis thaliana. *J. Cell Biol.* 172: 991–998.

Shimojima, M. and Ohta, H. (2011) Critical regulation of galactolipid synthesis controls membrane differentiation and remodeling in distinct plant organs and following environmental changes. *Progr. Lipid Res.* 50: 258–266.

Simon, M.L., Platre, M.P., Assil, S., van Wijk, R., Chen, W.Y., Chory, J., et al. (2014) A multi-colour/multi-affinity marker set to visualize phosphoinositide dynamics in Arabidopsis. *Plant J.* 77: 322–337.

Sousa, E., Kost, B. and Malho, R. (2008) Arabidopsis phosphatidylinositol-4-monophosphate 5-kinase 4 regulates pollen tube growth and polarity by modulating membrane recycling. *Plant Cell* 20: 3050–3064.

Stenzel, I., Ischebeck, T., Konig, S., Holubowska, A., Sporysz, M., Hause, B., et al. (2008) The type B phosphatidylinositol-4-phosphate 5-kinase 3 is essential for root hair formation in Arabidopsis thaliana. *Plant Cell* 20: 124–141.

Tejos, R., Sauer, M., Vanneste, S., Palacios-Gomez, M., Li, H., Heilmann, M., et al. (2014) Bipolar plasma membrane distribution of phosphoinositides and their requirement for auxin-mediated cell polarity and patterning in Arabidopsis. *Plant Cell* 26: 2114–2128.

Testerink, C. and Munnik, T. (2005) Phosphatidic acid: a multifunctional stress signaling lipid in plants. *Trends Plant Sci.* 10: 368–375.

Testerink, C. and Munnik, T. (2011) Molecular, cellular, and physiological responses to phosphatidic acid formation in plants. *J. Exp. Bot.* 62: 2349–2361.

Thole, J.M. and Nielsen, E. (2008) Phosphoinositides in plants: novel functions in membrane trafficking. *Curr. Opin. Plant Biol.* 11: 620–631.

Thole, J.M., Vermeer, J.E., Zhang, Y., Gadella, T.W., Jr. and Nielsen, E. (2008) ROOT HAIR DEFECTIVE4 encodes a phosphatidylinositol-4-phosphate phosphatase required for proper root hair development in Arabidopsis thaliana. *Plant Cell* 20: 381–395.

van Leeuwen, W., Vermeer, J.E., Gadella, T.W., Jr. and Munnik, T. (2007) Visualization of phosphatidylinositol 4,5-bisphosphate in the plasma membrane of suspension-cultured tobacco BY-2 cells and whole Arabidopsis seedlings. *Plant J.* 52: 1014–1026.

Vermeer, J.E. and Munnik, T. (2013) Using genetically encoded fluorescent reporters to image lipid signalling in living plants. *Methods Mol. Biol.* 1009: 283–289.

Vermeer, J.E., Thole, J.M., Goedhart, J., Nielsen, E., Munnik, T. and Gadella, T.W., Jr. (2009) Imaging phosphatidylinositol 4-phosphate dynamics in living plant cells. *Plant J.* 57: 356–372.

Vermeer, J.E., van Leeuwen, W., Tobena-Santamaria, R., Laxalt, A.M., Jones, D.R., Divecha, N., et al. (2006) Visualization of PtdIns3P dynamics in living plant cells. *Plant J.* 47: 687–700.

Vermeer, J.E., Van Munster, E.B., Vischer, N.O. and Gadella, T.W., Jr. (2004) Probing plasma membrane microdomains in cowpea protoplasts using lipidated GFP-fusion proteins and multimode FRET microscopy. *J. Microsc.* 214: 190–200.

Vincent, P., Chua, M., Nogue, F., Fairbrother, A., Mekeel, H., Xu, Y., et al. (2005) A Sec14p-nodulin domain phosphatidylinositol transfer protein polarizes membrane growth of Arabidopsis thaliana root hairs. *J. Cell Biol.* 168: 801–812.

Voigt, B., Timmers, A.C., Samaj, J., Hlavacka, A., Ueda, T., Preuss, M., et al. (2005) Actin-based motility of endosomes is linked to the polar tip growth of root hairs. *Eur. J. Cell Biol.* 84: 609–621.

Wada, Y., Kusano, H., Tsuge, T. and Aoyama, T. (2015) Phosphatidylinositol phosphate 5-kinase genes respond to phosphate deficiency for root hair elongation in Arabidopsis thaliana. *Plant J.* 81: 426–437.

Wimalasekera, R., Pejchar, P., Holk, A., Martinec, J. and Scherer, G.F. (2010) Plant phosphatidylcholine-hydrolyzing phospholipases C NPC3 and NPC4 with roles in root development and brassinolide signaling in Arabidopsis thaliana. *Mol. Plant* 3: 610–625.

Xue, H.W., Chen, X. and Mei, Y. (2009) Function and regulation of phospholipid signalling in plants. *Biochem. J.* 421: 145–156.

Yamaoka, Y., Yu, Y., Mizoi, J., Fujiki, Y., Saito, K., Nishijima, M., et al. (2011) PHOSPHATIDYLSERINE SYNTHASE1 is required for microspore development in Arabidopsis thaliana. *Plant J.* 67: 648–661.

Yeaman, C., Ayala, M.I., Wright, J.R., Bard, F., Bossard, C., Ang, A., et al. (2004) Protein kinase D regulates basolateral membrane protein exit from trans-Golgi network. *Nat. Cell Biol.* 6: 106–112.

Zhang, Y., Zhu, H., Zhang, Q., Li, M., Yan, M., Wang, R., et al. (2009) Phospholipase dalpha1 and phosphatidic acid regulate NADPH oxidase activity and production of reactive oxygen species in ABA-mediated stomatal closure in Arabidopsis. *Plant Cell* 21: 2357–2377.

Zhao, Y., Yan, A., Feijo, J.A., Furutani, M., Takenawa, T., Hwang, I., et al. (2010) Phosphoinositides regulate clathrin-dependent endocytosis at the tip of pollen tubes in Arabidopsis and tobacco. *Plant Cell* 22: 4031–4044.